

QUOKKA MANUAL

1. OVERVIEW

Quokka is a free software tool specialized for the fast simulation of silicon solar cell devices in one to three dimensions. It employs simplifications to the general semiconductor carrier transport model, which results in much less computational effort compared to alternative simulation software. Those simplifications, namely quasi-neutrality and conductive boundaries, are well validated to not impose notable loss of generality or accuracy for wafer-based silicon solar cell devices. Thus Quokka enables to simulate even moderately complex 3D silicon solar cell device geometries in short computation times on standard computers, while providing a similar level of accuracy and generality as state-of-the-art commercial device simulation software.

The main modelling difference to most other device simulation software comes with the conductive boundary simplification. Here near-surface regions, for example an emitter diffusion, are not modelled in detail by defining the doping profile and surface recombination etc. The inputs required are rather lumped properties of such regions, most importantly the sheet resistance and the effective recombination characteristic like for example the emitter saturation current density J_{0e} . This is well suitable if those inputs are the ones derived e.g. experimentally, but makes Quokka not (directly) applicable if for example an optimization of the doping profile is of interest.

Quokka essentially solves for the steady-state electrical characteristics of the device, and is capable to derive various typical solar cell characteristics: fixed terminal voltage, fixed terminal current, open-circuit (OC) conditions, maximum-power-point (MPP) conditions, short-circuit-current (J_{sc}) conditions, light- and dark-IV curve, quantum-efficiency (QE) curve, suns-Voc curve and series-resistance (R_s) curve. A notable extension is the inclusion of luminescence modelling, which allows Quokka to simulate for example spatially and spectrally resolved photo-luminescence characteristics.

While being powerful enough to simulate many silicon solar cell designs and conditions of practical interest, Quokka's scope is to be highly accessible for both newcomers and simulation experts. This is realized by the meshing and the solver numerics being largely automated and by using a pre-defined but flexible geometry layout, so that the required user inputs are reduced to a minimum and specifically designed for typical silicon solar cell conditions. Furthermore, Quokka automatically finds typical cell conditions of interest like maximum power point, and features an optimizer routine to fit unknown device properties to output characteristics. The software is hosted on pvlighthouse.com.au, where Quokka can be downloaded for free and support resources as well as a web-based settings file generator can be found.

Although these measures enable to perform extensive simulation tasks with little knowledge about fundamentals of numerical simulation, it is reminded that Quokka still is a full multidimensional solver with a large space of possible input combinations. As with any such complex tool the principle of "garbage in, garbage out" is still highly applicable, and limits of solvable conditions exist. In particular users intending to produce sensitive simulation results, for example for scientific publications, are strongly encouraged to follow the considerations in [Computational Performance and Accuracy](#).

2. INSTALLING AND RUNNING QUOKKA

2.1 INSTALLATION

Quokka is a compiled MATLAB program and requires the Matlab Comiler Runtime (MCR) 2013b to be installed. The MCR is freely available from the Mathworks website, be sure to download the correct (NOT the latest) version, 2013b:

<http://www.mathworks.com.au/products/compiler/mcr/index.html> (<http://www.mathworks.com.au/products/compiler/mcr/index.html>)

The latest Quokka version is available for download as Windows 32bit / 64bit, Linux and OSX version:

<http://www.pvlighthouse.com.au/resources/quokka2/quokka%202.aspx> (<http://www.pvlighthouse.com.au/resources/quokka2/quokka%202.aspx>)

The zip archive contains the Quokka executable as well as some example settings and input data files.

2.2 SETTINGS FILE AND PVL SETTINGS FILE GENERATOR

All settings required to define the simulation setup are given in the settings file. This is a Matlab script file (.m), which is however in ascii format and can therefore be modified with any text editor. While it is possible to directly edit the settings file, it is recommended to use the settings file generator on PVLighthouse, a web-based GUI which creates the settings file in a more user-friendly and less error-prone way:

<http://www.pvlighthouse.com.au/Resources/quokka2/quokka2%20settings%20file%20generator.aspx>
(<http://www.pvlighthouse.com.au/Resources/quokka2/quokka2%20settings%20file%20generator.aspx>)

Note that any input data files required for the simulation must be in the same directory as the settings file. Also all solution data will be stored in this directory.

2.3 RUNNING A SIMULATION

2.3.1 GUI

The easiest way to run the simulation is using the little GUI, which opens by default when starting Quokka.

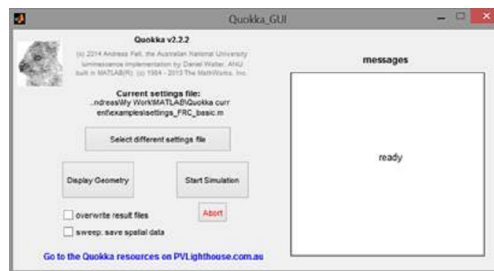


Figure 1: Quokka GUI

Table 1: Description of GUI Elements

GUI Element	Description and comments
Select different settings file	Browse and select one or multiple settings files. No reload is required when the settings file is modified.
Display Geometry	This is good practice to do before running the simulation as a quick sanity check for the geometry definition and resulting number of elements For multiple settings files only the first one will be displayed Sweep and optimizer settings are ignored In the Figure which opens up (see Figure 2) one can rotate and zoom, and toggle the visibility of selected features: xyz axis, F front side, R rear side, M metal coverage and S symmetry sides For multiple conductive boundaries of the same type a higher sheet resistance will be of lighter colour than the lower one, which can be useful for validating the arrangement of the respective boundaries The latter must not be mistaken with shaded colours, which indicates a contacted region
Start Simulation	Starts the simulation, plots and saves results if finished successfully Multiple settings files will be run sequentially

Abort	Aborts the simulation at selected points
	Only limited functionality for parallel simulations
Overwrite results files	When checked, Quokka will not append date and time to the result files
Sweep: save spatial data	When checked, Quokka will save all spatial data for each parameter during a sweep
Messages	Displays status and error messages

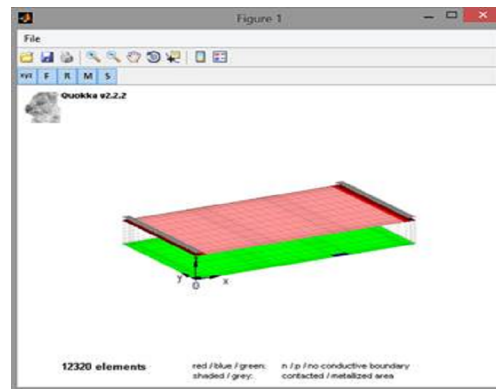


Figure 2: Geometry display figure

2.3.2 COMMAND LINE OPTIONS

When starting the Quokka executable from the command prompt, additional messages are displayed, and some additional functionality can be enabled by command line options, see Table 2.

For example, to run settings1.m and settings2.m parallelized on 5 CPUs in Windows:

```
Quokka2.exe cores5 settings1.m settings2.m
```

Starting those settings file in Linux as a background job without graphical output and redirecting command line output to nohup.out:

```
nohup ./Quokka2 cores5 no_display settings1.m settings2.m > nohup.out &
```

Table 2: Description of command line options

Command line option	Description and comments
*.m	Settings file to be simulated, *.m must be replaced by an actual unique filename Multiple settings files can be assigned and will be simulated sequentially; this saves the overhead to startup Quokka for each simulation
sweep_store_spatial_data	Quokka will save all spatial data for each parameter during a sweep
coresX	Enables parallel simulation mode, where X needs to be replaced by the desired number of parallel threads (max. 12 in Matlab 2013b) Only QE-curves, non-automatic IV-curves, sweeps and sequential optimization are executed in parallel, and the parallel mode will consequently not increase the speed of other simulations Limited messaging and abort functionality
no_display	Prevents the GUI and any graphic figures to open
overwrite_results	Quokka will not append date and time to the result files

sweep_store_spatial_data Quokka will save all spatial data for each parameter during a sweep

3. SETTINGS

3.1 BASIC CONCEPT

The input parameters are organized in several groups, which is loosely also reflected in the PVL settings file generator. These comprise **geom** (overall solution domain and contact geometry), **bulk** (bulk properties), **bound** (boundary conditions, i.e. diffusion and surface properties), **generation** (optics / generation), **circuit** (external circuit), **lumi** (luminescence modelling), **sweep** (parameter sweep) and **optim** (iterative optimization / curve fitting).

A standout input parameter is **circuit.terminal**, which controls at what operating point(s) the device will be simulated, and consequently what output characteristic is achieved. There is a qualitative difference between single operating point conditions, like a fixed terminal voltage, and “curves” consisting of many different operating conditions, like an IV-curve.

The sweep functionality sits “on top” and must be distinguished from the “curve” circuit.terminal options. If a curve terminal option is set together with a parameter sweep, the respective curve will be simulated for each sweep parameter.

The optimizer sits further “on top” on the sweep functionality, and the sweep can therefore not be used to run multiple optimizations with different input parameters. Such a “sequential optimization” must rather be defined using vector assignments to the **optim.override** inputs. The sweep can be used to create x-y value pairs for curve fitting. However, most common targets are readily produced by the curve terminal options, for example an IV curve by “IV_curve” and effective lifetime curve by “sunsVoc_curve”.

3.2 DESCRIPTION OF INPUT PARAMETERS

Table 3: Full list of input parameters, green and orange highlights parameters applicable only to FRC or IBC version, respectively; where applicable, default settings applied when no input is given are marked with an *

Parameter name	Units	Typical value range	Description	Applicability / dependencies
<i>GEOMETRY</i>				
version.design		‘FRC’ ‘IBC’	pre-defined geometry layout to use, see Predefined Layouts .	
geom.dimensions		1, 2 or 3	1D, 2D or 3D simulation	
geom.Wz	μm	50 ... 500	device thickness (z-direction)	
geom.Wx	μm	1 ... 10000	unit cell width in x-direction	2D and 3D only
geom.Wxfront	μm	1 ... 10000	front unit cell width in x-direction	if different, values must be integer and must have a reasonably low lcm, see Predefined Layouts .
geom.Wxrear	μm	1 ... 10000	rear unit cell width in x-direction	
geom.Wy	μm	1 ... 10000	unit cell width in y-direction	3D only

geom.frontcont.shape			'circle' 'rectangle' 'line' 'full'	shape of front (emitter) contact(s) in 2D, 'circle', 'rectangle' and 'line' produce identical geometry in 3D, 'line' will be orientated in y-direction	2D and 3D only
geom.rearcont.shape			'circle' 'rectangle' 'line' 'full'	shape of rear contact(s) in 2D, 'circle', 'rectangle' and 'line' produce identical geometry in 3D, 'line' will be orientated depending on the defined contact position, see Predefined Layouts .	2D and 3D only
geom.frontcont.wx	μm	1 ... 10000		half-width of front contact(s) in x-direction radius for 'circle'	2D and 3D only
geom.frontcont.wy	μm	1 ... 10000		half-width of front contact(s) in y-direction	3D only only for 'rectangle' contact shape
geom.rearcont.wx	μm	1 ... 10000		half-width of rear contact(s) radius for 'circle'	2D and 3D only
geom.rearcont.wy	μm	1 ... 10000		half-width of front contact(s) in y-direction	3D only only for 'rectangle' contact shape
geom.rearcont.position		[1] ... [1 3] ... [1 2 3 4]		vector with any combination of positions 1 to 4; defines the corner(s) where a rear contact exists, see Predefined Layouts ; all contacts have same shape and dimensions.	2D and 3D only positions 3 and 4 in 3D only
geom.leftcont.shape			'circle' 'rectangle' 'line'	shape of left (emitter) contact(s) in 2D, 'circle', 'rectangle' and 'line' produce identical geometry in 3D, 'line' will be orientated in y-direction	

geom.rightcont.shape			'circle' 'rectangle' 'line'	shape of right contact(s) in 2D, 'circle', 'rectangle' and 'line' produce identical geometry in 3D, 'line' will be orientated depending on the defined contact position, see Predefined Layouts .	
geom.lefttcont.wx	μm	1 ... 10000		half-width of left contact(s) in x-direction radius for 'circle'	
geom.leftcont.wy	μm	1 ... 10000		half-width of left contact(s) in y-direction	3D only only for 'rectangle' contact shape
geom.rightcont.wx	μm	1 ... 10000		half-width of right contact(s) radius for 'circle'	2D and 3D only
geom.rightcont.wy	μm	1 ... 10000		half-width of right contact(s) in y-direction	3D only only for 'rectangle' contact shape
geom.leftcont.numberx		0.5, 1, 1.5 ...		multiple of 0.5 defining the number of "half" left (emitter) contacts in x-direction within the unit cell, see Predefined Layouts .	
geom.leftcont.pitchx	μm	1 ... 1000		full pitch of multiple left (emitter) contacts within the unit cell	only for numberx > 0.5
geom.rightcont.numberx		0.5, 1, 1.5 ...		multiple of 0.5 defining the number of "half" right contacts in x-direction within the unit cell, see Predefined Layouts .	
geom.rightcont.pitchx	μm	1 ... 1000		full pitch of multiple right contacts within the unit cell	only for numberx > 0.5
geom.leftcont.w_metal	μm	0 ... 10000		left (emitter) metal half width, influences optics only	
geom.rightcont.w_metal	μm	0 ... 10000		right metal half width, influences optics only	

geom.leftcont.y_position			'aligned' 'opposite' 'double' 'half'	position of left (emitter) contact(s) relative to right contact(s) in y-direction, see Predefined Layouts .	3D only
geom.meshquality			1,2,3 or 'user'	1: coarse (sufficient for most simulations), 2: medium, 3: fine, 'user': use expert settings below	
geom.dzminfront	μm	0.2 ... 2		element size in z-direction at the front surface	for 'user' mesh quality only
geom.dzminfront	μm	0.2 ... 2		element size in z-direction at the rear surface	for 'user' mesh quality only
geom.dxmin	μm	0.2 ... 20		minimum element size in x-direction	2D and 3D only for 'user' mesh quality only
geom.dymin	μm	0.2 ... 20		minimum element size in y-direction	3D only for 'user' mesh quality only
geom.dxmax	μm	1 ... 500		maximum element size in x-direction	2D and 3D only for 'user' mesh quality only
geom.dymax	μm	1 ... 500		maximum element size in y-direction	3D only for 'user' mesh quality only
geom.scale		3 ... 20		determines minimum element sizes in x- and y-direction via dividing the smallest respective features (contact dimensions, gap etc.) by this number	2D and 3D only for 'user' mesh quality only
geom.inflation		1 ... 5		maximum allowable ratio of neighbouring element sizes; effectively controls how fast mesh sizes are increased away from feature edges	for 'user' mesh quality only

BULK PROPERTIES

Note that all recombination mechanisms are always active and additive, see [Quokka Physics](#)

bulk.type			'p-type' 'n-type'	doping type
bulk.rho	Ohm.cm	0.1 ... 1000		bulk resistivity

bulk.T	K	300K*	temperature; carefully check validity of applied models and inputs if changing temperature	
bulk.nk		'Green08_Nguyen14'* 'Green08_300K'	silicon optical properties, used for 1D_model generation and luminescence modeling	
bulk.mobility		'Klaassen'* 'Arora' 'Fixed'	mobility model, see Quokka Physics	
bulk.mun bulk.mup	cm ² /Vs		constant electron / hole mobility	'fixed' mobility only
bulk.nieff		'default'* 'fixed'	'default': see Quokka Physics 'fixed': user value	
bulk.nieffvalue	cm ⁻³	~1e10	fixed value of nieff	for 'fixed' bulk.nieff only
bulk.taub	μs	1 ... 1e5	fixed "background" bulk lifetime set to very high value (e.g. 1e10) to disable	
bulk.Auger		'Richter2012'* 'Altermatt2011' 'Kerr2002' 'Sinton1987' 'off'	Auger recombination model, see Quokka Physics	
bulk.Brad	cm ³ /s	4.73e-15*	radiative recombination coefficient set to 0 to disable radiative recombination	
bulk.SRH.BO.Nt	cm ⁻³	0* ... 1e18	oxygen concentration for BO-complex recombination, see Quokka Physics . delete or set to zero to disable	for p-type bulk only
bulk.SRH.BO.m		2 ... 4	processing dependent parameter for BO-complex recombination	for p-type bulk only
bulk.SRH.midgap.taun0	μs	1 ... 1e5	fundamental electron lifetime for midgap (defect level = Fermi level) SRH recombination	

bulk.SRH.midgap.taup0	μs	1 ... 1e5	fundamental hole lifetime for midgap (defect level = Fermi level) SRH recombination
bulk.SRH.custom{i}.Nt	cm^{-3}		defect density of i-th SRH defect
bulk.SRH.custom{i}.Et_Ei	eV	-0.5 ... 0.5	defect level of i-th SRH defect, relative to intrinsic energy
bulk.SRH.custom{i}.sigman	cm^2		electron capture cross section of i-th SRH defect
bulk.SRH.custom{i}.sigmap	cm^2		hole capture cross section of i-th SRH defect

BOUNDARY CONDITIONS

Index {i} stands for the i-th conductive- / nonconductive boundary condition, see [Defining Multiple Boundary Regions](#).

Each boundary can have a contacted and a non-contacted region with different recombination properties assigned to .cont. and .noncont, respectively

The IBC version does not support contacted non-conductive boundaries

bound.conduct{i}.location		'front' 'rear' 'left' 'right'	location of the i-th conductive boundary front and left located conductive boundaries are the "emitter" for FRC and IBC version, respectively	
bound.nonconduct{i}.location		'front' 'rear'	location of non-conductive boundary	
bound.conduct{i}.cont.rec bound.nonconduct{i}.cont.rec bound.conduct{i}.noncont.rec bound.nonconduct{i}.noncont.rec		'J0' 'S' 'expr'	How to model boundary recombination; by constant saturation current density J0, constant effective surface recombination velocity S or analytical expression	
bound.conduct{i}.cont.J0 bound.nonconduct{i}.cont.J0 bound.conduct{i}.noncont.J0 bound.nonconduct{i}.noncont.J0	A/cm²	0 ... 1e-10	saturation current density note the unit is A/cm², NOT fA/cm²	only for 'J0' recombination model

bound.conduct{i}.cont.S bound.nonconduct{i}.cont.S bound.conduct{i}.noncont.S bound.nonconduct{i}.noncont.S	cm/s	0 ... 1e6	effective surface recombination velocity 1e6 represents "infinite" recombination limited by carrier transport to the boundary; higher values therefore do not make any difference other than potentially causing numerical problems	only for 'S' recombination model
bound.conduct{i}.cont.expr bound.nonconduct{i}.cont.expr bound.conduct{i}.noncont.expr bound.nonconduct{i}.noncont.expr	A/cm ²	'expression'	analytical expression resulting in a boundary recombination current in A/cm ² Variables allowed to be used: dn : excess carrier density at the boundary in cm ⁻³ const.N : bulk doping density in cm ⁻³ const.nieff : bulk intrinsic carrier density in cm ⁻³ const.n0 : equilibrium minority carrier density in cm ⁻³ const.T : temperature in K const.Vt : thermal voltage in V const.q : elementary charge in As e.g.: '10*dn*const.q' (corresponds to Seff = 10 cm/s)	only for 'expr' recombination model
bound.conduct{i}.cont.J02 bound.nonconduct{i}.cont.J02 bound.conduct{i}.noncont.J02 bound.nonconduct{i}.noncont.J02	A/cm ²	0* ... 1e-6	n=2 saturation current density	only for 'J0' recombination model
bound.conduct{i}.type		'p-type' 'n-type'	conduction type of front conductive boundary in IBC version	
bound.conduct{i}.Rsheet	Ω	1 ... 10000	Sheet resistance	

bound.conduct{i}.shape			'full' 'line' 'rectangle' 'circle' 'contact'	shape of conductive boundary is always aligned to any contact(s) of the same type 'contact' sets the shape identical to the same type contact defined in the geometry group	2D and 3D only not applicable for IBC front conductive boundary (always full area)
bound.conduct{i}.wx	μm	1 ... 10000		width of conductive boundary in x-direction; radius for 'circle'	2D and 3D only
bound.conduct{i}.wy	μm	1 ... 10000		width of conductive boundary in y-direction	3D only 'rectangle' shape only
bound.conduct{i}.jctdepth	μm	0* ... 10		junction depth	
bound.conduct{i}.colleff			'fixed' 'ext_file'	how to model collection efficiency, see Quokka Physics	junction depth >0
bound.conduct{i}.colleff_value		0 ... 1*		fixed value for collection efficiency	'fixed' collection efficiency only
bound.conduct{i}.colleff_filename			'filename'	load collection efficiency from external file, see External File Format	'ext_file' collection efficiency only
<hr/> <i>GENERATION</i> <hr/>					
generation.type			'1D_model' 'Jgen_surface' 'Jgen_uniform' 'ext_file' 'customdata' 'off'	how to derive generation profile '1D_model': models generation profile by optical properties, see Quokka Physics 'Jgen_surface', 'Jgen_uniform': applies user-defined generation current to the illuminated surface or uniformly distributed through the device thickness	
generation.Jgen	mA/cm ²	~40		user defined total generation current	'Jgen_surface', 'Jgen_uniform' generation or with Jgen_correction=1

generation.jgen_correction		0* 1	1: scales the external or '1D_model' generation profile to match a desired total generation current defined by generation.jgen	'1D_model', 'ext_file' and 'customdata' generation only
generation.ext_file		'filename'	load generation profile from external file, see External File Format	'ext_file' generation only
generation.customdata	$\mu\text{m cm}^{-3}\text{s}^{-1}$	[z1, z2, ... zn; G1, G2, ... Gn]	generation profile with n value pairs; z: distance to illuminated surface G: generation rate	'customdata' generation only
generation.spectrum		'AM1.5g' 'monochromatic' 'custom'	defines the illumination spectrum	'1D_model' generation only
generation.monochromatic.wavelength	nm	250 ... 1450	monochromatic illumination wavelength	'monochromatic' spectrum only
generation.monochromatic.flux	$\text{cm}^{-2}\text{s}^{-1}$	$\sim 2\text{e}17$	photon flux of monochromatic illumination	'monochromatic' spectrum only
generation.facet_angle	°	0 or 54.7	facet angle of illuminated surface texture; set to 0 for planar surface	'1D_model' generation only
generation.spectrum_custom	nm $\text{Wm}^{-2}\text{nm}^{-1}$	[\lambda1, \lambda2, ... \lambda n; I1, I2, ... In]	custom spectrum with n value pairs: \lambda: wavelength I: spectral intensity	'custom' spectrum only
generation.transmission		'fixed' 'ext_file' 'custom'	how (wavelength dependent) transmission at the illuminated surface is defined 'fixed': fixed value for all wavelengths	'1D_model' generation only
generation.transmission_value		0 ... 1	fixed value for front transmission	'fixed' transmission only
generation.transmission_filename		'filename'	load front transmission data from external file, see External File Format	'ext_file' transmission only
generation.transmission_custom	nm	[\lambda1, \lambda2, ... \lambda n; T1, T2, ... Tn]	transmission curve with n value pairs: \lambda: wavelength T: transmission	'custom' transmission only

generation.Z		'fixed' 'ext_file' 'custom' 'param' 'limit_4n2' 'limit_Green02'	how (wavelength dependent) pathlength enhancement is defined	'1D_model' generation only
generation.Z_value		0 ... 1	fixed value for pathlength enhancement	'fixed' Z only
generation.Z_filename		'filename'	load pathlength enhancement data from external file, see External File Format	'ext_file' Z only
generation.Z_custom	nm	[$\lambda_1, \lambda_2, \dots \lambda_n$; Z1, Z2, ... Zn]	pathlength enhancement curve with n value pairs: λ : wavelength Z: pathlength enhancement	'custom' Z only
generation.Z0		1 ... 1000	Z0 for Z-parameterization	'param' Z only
generation.Zinf		1 ... 3	Zinf for Z-parameterization	'param' Z only
generation.Zp		1 ... 10	Zp for Z-parameterization	'param' Z only
generation.suns		0 ... 1 ... 10	scales the generation (AND intensity for efficiency calculation)	
generation.illum_side		'front' 'rear'	defines the illuminated side of the device	
generation.shading_width	μm	0 ... 10000	half shading width by metal fingers, independent of the contact width; Is applied as a line shading in y-direction centred to each contact on the illuminated side	2D and 3D only
generation.profile_type		'standard' 'cumulative'	'cumulative' expects PC1D-type profile	'ext_file' and 'customdata' only

EXTERNAL CIRCUIT

circuit.terminal

'Vuc' 'Vterm' 'Jterm'
'OC' 'MPP' 'Jsc'
'light_IV_auto'
'IV_curve' 'QE_curve'
'sunsVoc_curve'
'Rs_curve'

what "terminal"
condition to solve
**single operating
point conditions:**
'Vuc': fixed unit cell
voltage (fastest
because no
iterations required)
'Vterm': fixed
terminal voltage
'Jterm': fixed
terminal current
'OC': open-circuit (do
NOT set high series /
contact resistance as
in PC1D) 'MPP':
maximum power
point 'Jsc': short-
circuit-current (NOT
short-circuit, voltage
will be >0, but
extracted current
will be Jsc) **"curve"**
terminal condition:
'light_IV_auto':
automated algorithm
to quickly but
accurately derive
light IV-curve and
parameters (Voc, Jsc,
FF, eta) 'IV_curve':
solve at multiple
user defined
voltages 'QE_curve':
quantum efficiency
at multiple user
defined wavelengths
'sunsVoc_curve':
solve at multiple
user defined
suns-values
'Rs_curve': extract
voltage dependent
series resistance via
double-light method;
solves two
automated light-IV
curves with slightly
different generation;
advice: set
circuit.IV_accuracy to
at least 5 for smooth
and accurate results

circuit.Vuc.value

V

0.3 ... 1

unit cell voltage
(BEFORE external
circuit elements);
avoid values close to
zero, see Short-
circuit Limitations

'Vuc' terminal
only

circuit.Vterm.value	V	0.3 ... 1	terminal voltage (AFTER external circuit elements); avoid values close to zero, see Short-circuit Limitations	'Vterm' terminal only
circuit.Jterm.value	mA/cm ²	-40 ... 1000	terminal current	'Jterm' terminal only
circuit.IV.mode		'Vterm' 'Vuc'	whether to define unit cell (faster) or terminal voltages (slower) for IV_curve solution	'IV_curve' terminal only
circuit.IV.V_values	V	[V1, V2, ... Vn]	n voltage values for IV_curve	'IV_curve' terminal only
circuit.IV.init_previous		0* 1	1: use solution from previous results as starting guess; faster and more stable for closely spaced IV points; disables parallel simulation of IV-curve 0: initialize start values for each IV point; more robust for largely spaced IV points	'IV_curve' terminal only
circuit.QE.wavelength_values	nm	[λ1, λ2, ... λn]	n wavelength values for QE_curve	'QE_curve' terminal only
circuit.sunsVoc.suns_values		[s1, s2, ... sn]	n suns values for sunsVoc_curve	'sunsVoc_curve' terminal only
circuit.DJ0	A/cm ²	0*... 1e-7	saturation current density of external diode, see Quokka Physics	requires circuit.Dn
circuit.Dn		1 ... 4	ideality factor of external diode, see Quokka Physics	required if circuit.DJ0 is defined
circuit.Voc_guess	V	0.67*	guess of Voc for iteration starting point; better guess can speed up the simulation	'OC', 'MPP' and 'light_IV_auto' terminal only

circuit.IV_accuracy	1* ... 10	higher value increases the number of points simulated on the light IV-curve does NOT influence the accuracy of IV-curve parameters (Voc, Jsc, FF, eta) >= 5 is recommended for 'Rs_curve' terminal option	'light_IV_auto' and 'Rs_curve' terminal only
---------------------	-----------	---	--

LUMINESCENCE MODELLING

For luminescence modelling "front" always refers to the detection side which could actually be the rear side

lumi.enable	1 0	switch luminescence on (1) or off (0) if off, no further inputs are required	
lumi.scale	a.u.	simply scales the simulated luminescence signal can be used to convert simulated detected photon flux into measurement units, e.g. counts/s	
lumi.normalize_signal	1 0	whether to normalize (1) the simulated signal or not (0); will normalize the spectrum and / or intensity map to its respective peak value	
lumi.detection_side	'illuminated' 'opposite'	whether the sensor detects luminescence from the illuminated or non-illuminated side	
lumi.filter	'none' 'ext_file'	how to define wavelength dependent transmission from the sample surface to the sensor (i.e. lens and filter transmission) 'none': 100% transmission	
lumi.filter_filename	'filename'	load optics transmission data from external file, see External File Format	'ext_file' filter only

lumi.sensor_EQE			'unity' 'silicon' 'ext_file'	how to define wavelength dependent external quantum efficiency of sensor 'unity': 100% EQE 'silicon': calculates EQE assuming Lambert-Beer-Law for absorption with silicon absorption coefficient and sensor thickness	
lumi.sensor_thickness	μm			thickness of sensor for calculation of EQE; more correctly, this is the total pathlength which is directly inserted into the Lambert-Beer-Law	'silicon' sensor EQE only
lumi.sensor_EQE_filename			'filename'	load sensor EQE from external file, see External File Format	'ext_file' sensor EQE only
lumi.wavelength_start	nm	800* ... 1400		lower bound of wavelength to include into modeling	
lumi.wavelength_end	nm	800 ... 1400*		upper bound of wavelength to include into modeling	

lumi.emission_function		1 2 3 4	how to model internal optics, see Quokka Physics 1 : both sides planar, quasi-1D 2: both sides textured, quasi-1D 3: general, quasi-1D; further inputs required, see below; set of default values approximately applicable for typical textured front and semi-planar rear solar cell devices 4: both sides lambertian, 2D and 3D geometrical blurring; user-defined mesh settings with relatively low dxmax (and dymax) recommended for smooth and accurate results; can be highly computationally intensive	4: 2D and 3D only
lumi.internal_refl		'default' 'ext_file'	how to define wavelength dependent internal surface reflectivity 'default': assumes planar silicon – air interface on both sides	not applicable for emission function 2
lumi.internal_refl_filename		'filename'	load internal reflectivity for front and rear surface from external file, see External File Format	'ext_file' internal reflectivity only
lumi.general.facet_angle	°	0 ... 54.7	facet angle of front surface texture set to zero for planar surface	emission function 3 only
lumi.general.lambertian_factor		0 ... 1	lambertian factor of rear side 0: completely specular 1: completely diffuse	emission function 3 only
lumi.general.refRear		0 ... 0.6* ... 1	internal rear reflectivity	emission function 3 only
lumi.general.refFrontS		0 ... 0.62* ... 1	first internal front reflectivity	emission function 3 only

lumi.general.refFrontN	0 ... 0.93* ... 1	n-th internal front reflectivity	emission function 3 only
lumi.geometrical.number_reflections	0 ... 20	number of internal reflections to trace high number might add significant computational effort	emission function 4 only

PARAMETER SWEEP

Index {i} stands for the i-th dependent sweep parameter

All dependent sweep parameters must have the same number of values

To have only one independent (group of) sweep parameter(s), assign values only to one (group) (..._1 or ..._2)

sweep.enable	1 0	switch parameter sweep on (1) or off (0) if off, no further inputs are required	
sweep.param_1{i} sweep.param_2{i}	'input parameter'	input parameter to sweep within the first / second independent group of sweep parameters, e.g.: 'bulk.rho' must exactly match an input parameter existing within the settings file	
sweep.values_1{i} sweep.values_2{i}	same as i-th sweep parameter	[v1, v2, ... vn] {'S1', 'S2', ... 'Sn'}	sweep values for i-th sweep parameter of the first / second independent group of sweep parameters can be numeric (v) or strings (S) sweeping of some string values including external file names NOT possible yet to disable the second (group of) independent sweep parameter(s): sweep.value_2{1}=[];

OPTIMIZER

Index {i} stands for the i-th parameter to optimize / the i-th goal to achieve / the i-th override rule to apply

For sequential optimization, each vector input must have the same length n

optim.enable	2 1 0	switch off / change mode of optimizer 2: curve fitting mode 1: goal mode 0: off; not further input required	
--------------	-------	---	--

optim.maxiter		5 ... 50	maximum number of iterations; aborts once this number is reached	
optim.accuracy		0.1 ... 1* ... 10	influence termination tolerances higher values potentially increases accuracy but at the cost of increased number of iterations and increased likelihood of “stuck” optimizations	
optim.param{i}		‘input parameter’	input parameter to optimize, e.g.: ‘bulk.rho’ must exactly match an input parameter existing within the settings file	
optim.start{i}	same as i-th optim. parameter	same as i-th optim. parameter	start value of parameter to optimize should be carefully chosen not far from the final result for good convergence	
optim.lb{i}	same as i-th optim. parameter	same as i-th optim. parameter	lower bound of allowed values for parameter to optimize <optim.start{i}	
optim.ub{i}	same as i-th optim. parameter	same as i-th optim. parameter	upper bound of allowed values for parameter to optimize >optim.start{i}	
optim.goal{i}		‘scalar result’ e.g. ‘results.eta’	name of i-th goal to achieve; must be a scalar within the results structure produced by the simulation setup, see Table 5	mode 1 only
optim.value{i}	same as scalar result defined in i-th goal	‘max’ ‘min’ v [v1, v2, ... vn]	value of i-th goal to achieve; ‘max’: maximises the result ‘min’: minimises the result v: (vector of) numerical value(s)	mode 1 only ‘min’ and ‘max’ only for a single goal i=1

optim.goalsx	'vector result' e.g. 'results.curves .navg'	name of x-values to achieve must be a vector within the results structure produced by the simulation setup, see Table 5	mode 2 only
optim.goaly	'vector result' e.g. 'results.curves .taueff'	name of y-values to achieve must be a vector within the results structure produced by the simulation setup with the same length as the one defined in optim.goalsx, see Table 5	mode 2 only
optim.xyfile	'filename'	external file containing x-y-value pairs which define the target curve to fit to	mode 2 only
optim.override.param{i}	'input parameter'	name of i-th parameter to override during the optimization	
optim.override.value{i}	'expression' v [v1, v2, ... vn]	override value to assign during the optimization 'expression': analytical expression containing the parameter(s) to optimize, e.g.: 'bulk.rho*5' v: (vector of) numerical value(s)	

4. DATA INPUT / OUTPUT

4.1 EXTERNAL FILE FORMAT

Several inputs like for example a generation profile can be defined via external files. Those files must be located in the same directory as the settings file and the containing data must be correctly organized to be usable by Quokka.

Accepted file formats are either Excel files (.xls or .xlsx) or ASCII files (.txt or .csv). Note that only "proper" Excel files can be read, while those produced with alternative tools, like for example by the PVLighthouse website, can cause reading errors. This can be fixed by opening and saving them in Excel. For the ASCII files, most common delimiters are supported. Furthermore, a comma decimal separator is supported, which takes slightly longer to import due to internal string replacement.

The data must be organized in columns, where the first two (three) columns contain the input data and the first row can optionally be a header row or the first data row. Table 4 summarizes the data organization for the different external file inputs.

Table 4: Data organization in external files

Assigned to input parameter	First column	Second column	Third column
generation.ext_file	distance to illuminated surface in μm	generation rate in $\text{cm}^{-3}\text{s}^{-1}$	
generation.transmission_filename	wavelength in nm	front transmission 0 ... 1	
generation.Z_filename	wavelength in nm	pathlength enhancement Z	
bound.conduct{i}.colleff_filename	wavelength in nm	collection efficiency 0 ... 1	
lumi.filter_filename	wavelength in nm	transmission 0 ... 1	
lumi.sensor_EQE_filename	wavelength in nm	EQE 0 ... 1	
lumi.internal_refl_filename	wavelength in nm	front reflectivity 0 ... 1	rear reflectivity 0 ... 1
optim.xyfile	same quantity and unit as defined in optim.goalx	same quantity and unit as defined in optim.goaly	

4.2 DATA OUTPUT

Naturally, what output data is available depends on what characteristics the device is solved for. A basic distinction is between single operating point and multiple operating points characteristics. Only for a single operating point a unique electrical condition with unique spatial results, including luminescence results, is present and will be stored. This is not the case for the curve terminal conditions 'IV_curve', 'sunsVoc_curve' and 'Rs_curve', and consequently no spatial and luminescence output is available. Outstanding operating points exist for 'light_IV_auto' (maximum power point) and 'QE_curve' (short circuit current conditions) and therefore spatial data is available for those, as well as for all single operating point terminal conditions 'Vuc', 'Vterm', 'Jterm', 'OC', 'MPP' and 'Jsc'.

When a sweep is performed, no spatial data will be available by default, however can be stored for each parameter by activating the corresponding switch, see [Running A Simulation](#).

4.2.1 GRAPHICAL OUTPUT

The kind of graphical output is predefined and dependent on what terminal condition was solved, and whether a sweep or optimization task was performed. Spatial data will only be plotted when a single point terminal condition was set, respective curves will be shown for curve terminal conditions, and the variation of few major scalar outputs for a parameter sweep. Beyond that, there is no influence by the user on the graphical output. All important results are stored in a csv and Matlab file, the latter containing also spatial output if applicable, from which users must create custom graphics themselves.

4.2.2 RESULTS FILES

Quokka saves two results files, a .csv file containing most scalar and curve outputs, and a .mat file containing additional results including spatial output data (if available). The .mat file is a Matlab file format, which can be read by several software tools, but is naturally best processed in Matlab. If the optimizer is used, the results will be saved in files which include 'optim' in the file name (with some additional outputs not listed below).

Table 5: List of output quantities contained in the .csv and / or .mat results file; nomenclature according to .mat file, .csv file is equivalent

Output quantity	Units	Description
<i>SCALAR OUTPUTS</i>		
Vterm	mV	terminal voltage (including external circuit elements)
Jterm	mA/cm^2	terminal current density (including external circuit elements)

Vuc	mV	unit cell voltage (excluding external circuit elements)
Juc	mA/cm ²	unit cell current density (excluding external circuit elements)
Voc	mV	open circuit voltage (@ 1 sun for suns-Voc curve)
Jsc	mA/cm ²	short-circuit current density (total generation current density @ 1 sun for suns-Voc curve)
FF	%	fill factor of light-IV curve (pseudo fill factor for suns-Voc curve)
eta	%	efficiency (pseudo efficiency for suns-Voc curve)
Vmpp	mV	terminal voltage at maximum power point
Jmpp	mA/cm ²	terminal current density at maximum power point
navg	cm ⁻³	average minority carrier density
taueff	μs	effective lifetime, definition see Quokka Physics
conduct	S	excess conductivity, definition see Quokka Physics
JL_two_diode	mA/cm ²	current density source from two-diode model fit
J01_two_diode	A/cm ²	ideal saturation current density from two-diode model fit
J02_two_diode	A/cm ²	non-ideal (n=2) saturation current density from two-diode model fit
Rseries_two_diode	Ωcm ²	series resistance from two-diode model fit
Rshunt_two_diode	Ωcm ²	shunt resistance from two-diode model fit
Rseries_mpp_pow	Ωcm ²	series resistance @ MPP from power loss, definition see Quokka Physics
Rseries_mpp_DLM	Ωcm ²	series resistance @ MPP from double light method
lumi_mean	a.u.	average luminescence signal (detected photon flux times scaling factor)
computing_time	s	total computing time (not correct when optimizer is used)
JGbulk	mA/cm ²	generation current density of the bulk
JGfront	mA/cm ²	generation current density of the front conductive boundaries
JGfront	mA/cm ²	generation current density of the rear conductive boundaries
N	cm ⁻³	bulk doping density
nieff	cm ⁻³	effective intrinsic carrier density
n0	cm ⁻³	equilibrium minority carrier density

FELA OUTPUTS (SEE QUOKKA PHYSICS FOR DEFINITIONS)

FELA.gen	mW/cm ²	generated power
FELA.res_bulk_n	mW/cm ²	resistive loss from electron transport in the bulk
FELA.res_bulk_p	mW/cm ²	resistive loss from hole transport in the bulk
FELA.res_front_conduct FELA.res_left_conduct	mW/cm ²	resistive loss in the front / left conductive boundary(ies)
FELA.res_front_cont FELA.res_left_cont	mW/cm ²	resistive loss from front / left contact resistance
FELA.res_rear_conduct FELA.res_right_conduct	mW/cm ²	resistive loss in the rear / right conductive boundary(ies)
FELA.res_rear_cont FELA.res_right_cont	mW/cm ²	resistive loss from rear / right contact resistance
FELA.res_front	mW/cm ²	IBC only: resistive loss in the front conductive boundary
FELA.rec_Auger	mW/cm ²	intrinsic bulk recombination loss (Auger and radiative)
FELA.rec_SRH	mW/cm ²	other bulk recombination loss (SRH and fixed bulk lifetime contributions)
FELA.rec_front_conduct FELA.rec_left_conduct	mW/cm ²	recombination in the front /left conductive boundary(ies), includes loss due to non-optimal collection efficiency
FELA.rec_front_cont FELA.rec_left_cont	mW/cm ²	recombination at the front / left contacts
FELA.rec_rear_conduct FELA.rec_right_conduct	mW/cm ²	recombination in the rear / right conductive boundary(ies), includes loss due to non-optimal collection efficiency
FELA.rec_rear_cont FELA.rec_right_cont	mW/cm ²	recombination at the rear / right contacts
FELA.rec_front_nonconduct	mW/cm ²	recombination in the front non-conductive boundary
FELA.rec_rear_nonconduct	mW/cm ²	recombination in the rear non-conductive boundary
FELA.ext_series	mW/cm ²	loss at the external series resistance
FELA.ext_shunt	mW/cm ²	loss at the external shunt resistance
FELA.ext_diode	mW/cm ²	loss at the external diode
FELA.error	%	FELA balance error, see Verify Accuracy

CURVE OUTPUTS

curves.Vterm	mV	terminal voltage (including external circuit elements)
curves.Jterm	mA/cm ²	terminal current density (including external circuit elements)
curves.Vuc	mV	unit cell voltage (excluding external circuit elements)

curves.Juc	mA/cm ²	unit cell current density (excluding external circuit elements)
curves.QE_lambda	nm	wavelength values for QE curve
curves.CE	%	collection efficiency, definition see Quokka Physics
curves.IQE	%	internal quantum efficiency
curves.EQE	%	external quantum efficiency
curves.suns	suns	values for suns-Voc curve
curves.Voc	mV	open circuit voltage
curves.navg	cm-3	average minority carrier density
curves.taueff	μs	effective lifetime, definition see Quokka Physics
curves.Vi	mV	terminal voltage, finely spaced values for Rs-curve
curves.Rseries_DLM	Ωcm ²	series resistance from double light method
<i>MAIN SPATIAL OUTPUTS</i>		
grid.XX / YY / ZZ	m	vector with coordinate values of grid
grid.X / Y / Z	m	3D array with coordinate values of grid
grid.dx / dy / dz	m	3D array with elements sizes
spatial.dn	cm-3	3D array of excess carrier density
spatial.nfront / nrear	cm-3	2D array of excess carrier density at the front / rear boundary
spatial.QFn / QFp	V	3D array of electron / hole quasi-Fermi potential
spatial.Pel	V	3D array of electric potential
spatial.Ffront / Frear	V	2D array of potential in front / rear conductive boundary(ies)
spatial.G	cm-3s-1	3D array of bulk generation rate
spatial.R	cm-3s-1	3D array of bulk recombination rate (sum of all contributions)
spatial.Jnx / Jny / Jnz mA/cm ²	3D array of electron current density component	These are defined at element faces and therefore contain one more value in each coordinate direction than other 3D arrays
spatial.Jpx / Jpy / Jpz mA/cm ²	3D array of hole current density component	These are defined at element faces and therefore contain one more value in each coordinate direction than other 3D arrays
spatial.sigman / sigmap	S/cm	3D array of electron / hole conductivity
spatial.Jrec3	mA/cm ²	3D array of recombination current density at solution domain boundaries (contains non-zero values at outer elements only)

5. COMPUTATIONAL PERFORMANCE AND ACCURACY

5.1 GENERAL COMMENTS ON PERFORMANCE

Quokka's (relative) ease of set-up, speed and capability for extensive sweep and optimizing tasks was found to raise expectations on stability and convergence compared to more complex tools. It is therefore reminded that this is still a full multidimensional simulation tool allowing for a wide range of conditions, so convergence naturally is a challenging topic. Yet Quokka, due to its simplifications and specialization, actually is more robust and faster for the conditions it is designed for than full device simulators.

Quokka's numeric are designed and optimized for typical solar cell conditions, and bad or no convergence can be expected for very badly performing cell structures, exotic test structures or extreme conditions. This should especially be considered when using large parameter sweeps which may cover such extreme conditions. Quokka's philosophy is to keep settings simple and don't allow users "messing around" too much (potentially producing wrong results), therefore there is limited possibility for the user to tweak numerics.

In general, finer mesh quality gives higher accuracy at the cost of computational time. It must be considered however, that a finer mesh in general also worsens convergence. Usually this results in a crash, but potentially also leads to a solution with low accuracy.

5.2 VERIFY NUMERICAL ACCURACY

While meshing in Quokka is largely automated and even the coarse mesh setting will yield acceptable accuracy in many cases, verifying numerical accuracy is ultimately the responsibility of the user. The comments below give hints on how to judge and reach numerical accuracy:

- The command line output from Matlab's `fsolve` function sometimes says "inaccuracy possible" or "no solution found". In most cases the result is still accurate, with the warning resulting from tight termination criteria on the derived SNLE, which are only loosely related to the relevant solution accuracy.
- The FELA balance, see [Quokka Physics](#), gives a good indication of the overall quality of convergence, and should be roughly less than 1%. However, a low fela balance is not sufficient evidence for low numerical error, as it does not necessarily include discretization errors. On the other hand, many scalar results might still be accurate even when a high fela balance is present.
- For sensitive results it is mandatory to check for numerical accuracy by verifying mesh independency. That means a desired result is accurate if it shows negligible difference when using a significantly different (usually finer) mesh. If both, mesh independency of key scalar results and a low fela balance is achieved, one can safely assume good overall numerical accuracy.

5.3 SHORT-CIRCUIT LIMITATIONS

Conditions with illumination and close to short circuit are challenging because of the physically existing large gradients. In particular the relatively coarse mesh close to the surface compared to other device simulators, as a result of the conductive boundary simplification, may lead to significant inaccuracies and/or convergence issues in Quokka. A finer mesh increases accuracy but can also worsen the convergence. It is strongly advised to avoid voltages close to zero, i.e. $V_{oc} < \sim 200$ mV. For representing short-circuit conditions it is usually sufficient to use higher voltages which still extract J_{sc} . This is what Quokka does for automatic light-IV and J_{sc} terminal conditions, and is an important consideration when performing a manual light-IV curve.

A typical numerical artefact related to this short-circuit inaccuracy is an apparent minimum of the current density at around 100 mV – 300 mV of the light-IV curve, with the minimum value being closest to the actual J_{sc} value.

5.4 LUMINESCENCE MODELLING

The statistical escape function models 1 – 3 come with negligible computational effort relative to the device simulation. For an accurate spectrum, a finer z-resolution of the mesh may be required, which is up to the user to check and verify.

The geometrical blurring model 4 can be computationally more expensive than the electrical simulation, in particular in 3D. Significant inaccuracy in spatial results can be present if large lateral element sizes are set, observable by unphysical peaks and non-smooth results. To overcome this, the use of expert mesh settings with small `geom.dxmax` and `geom.dymax` is recommended. Another source of inaccuracy is present when the typical "blurring length" is in the order of the unit cell width. More than one repetition of the unit cell would be necessary, which would however be computationally expensive.

and is so far not implemented. Also note that this blurring model has not yet been extensively validated and results should be interpreted and used with care.

5.5 OPTIMIZER

Using the optimizer functionality in Quokka means iteratively performing full numerical device modelling within a large parameter space. As with any such complex and potentially strongly non-linear function to optimize, it is of high importance to carefully setup the optimization task. This comprises choosing sensible start values for the parameter(s) to optimize, tight upper and lower bounds to it, and having the confidence that the optimal value is within the bounds and that the target is sufficiently sensitive to the parameter(s) to optimize. Furthermore, the number of parameters and goals, though in principle unlimited, should be limited to a minimum, to prevent bad convergence and / or finding of local rather than global minima. For example, while choosing more than two or three input parameters as unknown's to maximise efficiency is easily set up, it will hardly converge to the true global maximum, unless the start values are already very close to the solution. For curve fitting, care needs to be taken by the user to ensure overlapping of the user-defined and simulated x-values within the given bounds of the unknown parameter, as least-squares calculation can only be performed in the overlapping region.

6. DESCRIPTION OF KEY FUNCTIONALITY

6.1 GEOMETRY DEFINITION AND MESHING

6.1.1 PRE-DEFINED LAYOUTS: FRC AND IBC VERSION

As mentioned, Quokkas scope is to only provide a minimum number of input parameters to define and solve typical wafer based silicon solar cell devices. Being the main task for most multidimensional device simulations, Quokka is restricted to solve an element of symmetry or 'unit cell', which means that the sides (2 sides in 2D, 4 in 3D) are always set to symmetry boundary conditions. Furthermore, coarsely pre-defined geometry layouts are used, with the flexibility to change relevant dimensions and contact patterns. However, this means that Quokka's input capabilities do not allow the definition of arbitrary device geometries. The two supported layouts are called 'front and rear contact' (**FRC**) and 'interdigitated back contact' (**IBC**) version.

The **FRC** version fixes the front to only have contacts and conductive boundary types of opposite polarity to the bulk, and at the rear of the same polarity, respectively. In other words, all emitter diffusions and emitter contacts must be located at the front, and all base contacts on the rear. Rear emitter cells can still be simulated by setting illumination to the rear. The FRC version features multiple rear contacts located at any of the unit cell corners / edges, which allows for example to define a hexagonal rear contact pattern. Furthermore it supports a different unit cell width in x-direction for the front and the rear side. This effectively means that one can define a different front and rear contact pitch. This results not in a valid unit cell geometry, which Quokka handles by repeatedly stitching the front and rear geometry until they exactly match up. This larger valid unit cell has an x-dimension which is equal to the least common multiplier (LCM) of the defined front and rear width. This means that no arbitrary numbers should be chosen which could result in extremely large solution domains, but care has to be taken by the user to ensure a reasonably low LCM.

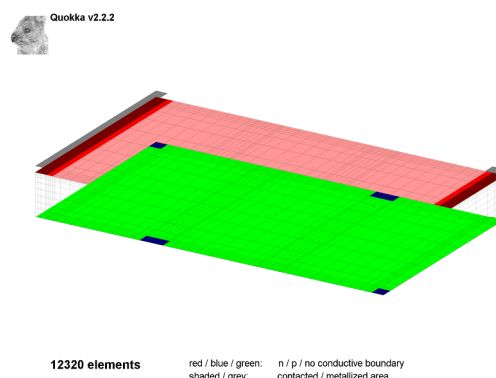


Figure 3: Example FRC geometry featuring a selective emitter at the front and hexagonal LBSF at the rear; note the different unit cell widths at front and rear, which results in a larger solution domain width equal to the LCM.

The **IBC** versions has both polarity contacts on the rear, and no contacts on the front. It is organized in such way that the opposite polarity conductive boundaries and contacts ('emitter') are always positioned at the left side, and the respective base features on the right side. Within the IBC unit cell one can define an arbitrary number of in x-direction equally spaced and shaped contacts for the left and right side independently. For 3D no such feature is available in y-direction, here it can only be defined whether the contacts are positioned at one or both of the edges.

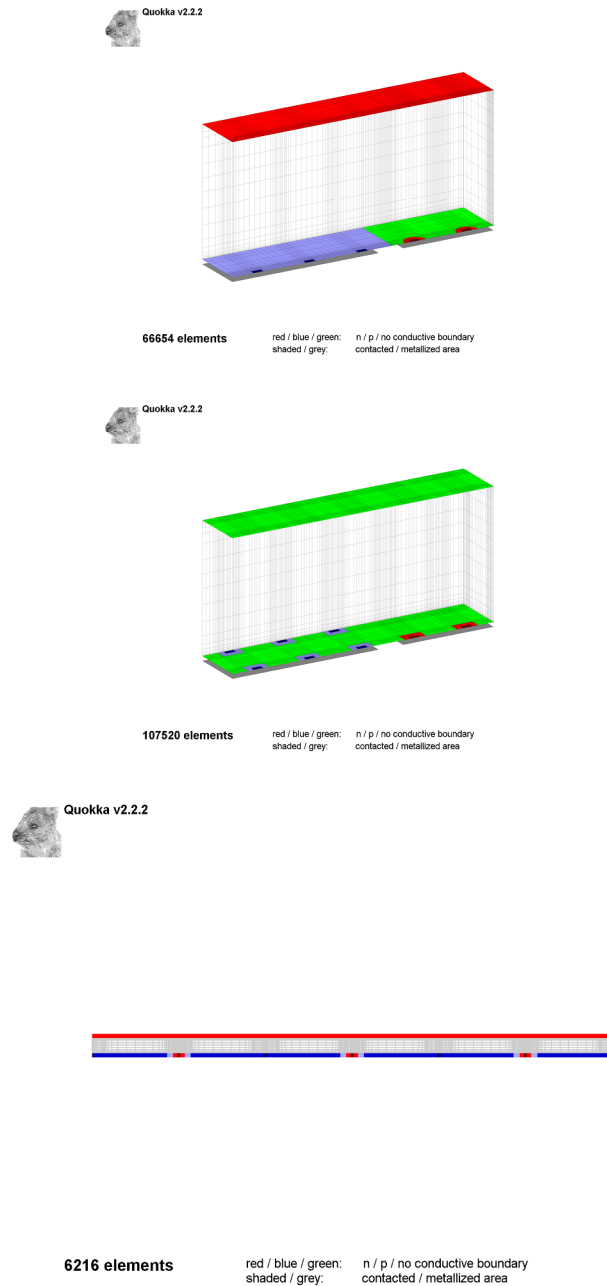


Figure 4: Example IBC geometries produced by Quokka; upper left: large area p+ region (emitter) with localized circular n+ regions, and localized contact openings; upper right: point-contact design; lower: large 2D solution domain containing multiple repetitions of symmetry element.

6.1.2 DEFINING MULTIPLE BOUNDARY REGIONS

Quokka allows to define an arbitrary number of conductive boundaries with different shapes and properties by indexing. In areas where conductive boundaries overlap, the one with the highest index is applied. Their centre position is always aligned to every contact at the respective side (front / rear for FRC, left / right for IBC). An exception exists in the IBC version: if the width of a conductive boundary is larger than the x-pitch of the respective contacts, it is centred at the respective edge of the solution domain (left / right). Adjacent conductive boundaries of the same type are electrically connected. In regions where no conductive boundary is applied, properties for the non-conductive boundary are applied. Figure 5 illustrates this functionality.



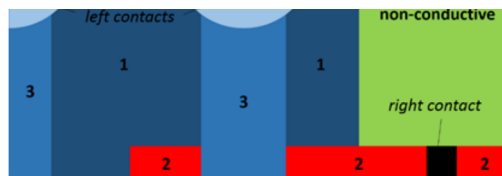


Figure 5: (non-sensible) example to illustrate definition of multiple conductive boundaries; IBC rear side with opposite contact positions and 4 conductive boundaries, one 'right' (#2: n+ BSF) and 3 'left' conductive boundaries (#1, #3, #4: p+ emitter); boundaries #1 and #2 are wider than the respective contact pitch and are therefore centred at the left and right solution domain edge, respectively, whereas boundaries #3 and #4 are centred at the respective contacts.

6.1.3 MESHING INSIGHTS

Quokka uses an orthogonal, non-equidistant mesh for discretization of the solution domain, which is well suited for the typically cuboidal shapes of silicon solar cell devices. The automated meshing algorithm works as follows: first, a minimum element size in each coordinate direction is determined from the minimum of either the user input or the minimum feature / gap size divided by a user-defined scale factor. This minimum element size is applied to all feature edges, including front and rear side, but NOT the symmetry sides. From there the mesh is inflated where the size of adjacent elements is increased by the inflation factor. Typical settings for scale factor, inflation factor and minimum element sizes are pre-defined in the mesh-quality settings 1 (coarse), 2 (medium) and 3 (fine), and can further be defined by the user. Note that for many purposes a 'coarse' mesh will yield acceptably accurate results, and is the recommended initial setting due to numerical speed and robustness. However, mesh independency should be verified for sensitive results, see [Verify Accuracy](#).

A complication arises when different junction depths for conductive boundaries are defined. The physical solution domain in Quokka covers the quasi-neutral region only, i.e. excludes the junction depths. At the same time the cuboidal solution domain can only accept a unique value for its size in z-direction. Quokka handles this by setting the solution domain size to the **defined thickness less the area-average junction depth**, see Figure 6. Care is taken to use the originally defined junction depths when calculating the generated and collected current in the boundary, and compensating for the spatial gap / overlap by accordingly adjusting the generation in the bulk next to the boundary. This approach is accurate if the junction depths are much smaller than the device thickness and the size of the conductive boundaries.



Figure 6: Illustration of solution domain thickness reduction by the area-average junction depth.

6.1.4 BOTH POLARITY CONTACTS ARE ALWAYS REQUIRED

The solver algorithm in Quokka requires a voltage to be applied, which makes the **definition of both polarity contacts a fundamental requirement**. Often it is desirable to simulate test structures without contacts, i.e. lifetime or photoluminescence test structures. This can still be done in Quokka by defining 'virtual contacts' and solving for open circuit conditions. If the properties of the virtual contacts are defined in a way that they represent non-contacted regions, their influence at open circuit eventually vanishes and the simulation represents a sample without any contacts. This is achieved by setting recombination of the contacted region equal to the non-contacted region it represents, and choosing a small contact size to not significantly suppress lateral gradients by pinning the respective quasi-Fermi-potential to the constant voltage of the boundary. However, the virtual contact should not be too small to prevent extremely small element sizes and consequently high computational effort. A typically good value for the size of the virtual contact is a few percent of the solution domain size.

6.2 VARYING INPUT PARAMETERS: SWEEP AND OPTIMIZER

6.2.1 SWEEP

Quokka has the built-in functionality to perform parameter sweeps. It can sweep one or two independent groups of dependent parameters indexed. Here, **dependent parameters** mean that both must have the same number of values, which is the number of simulations to be performed using the defined value pairs, and are indexed in the settings file by curly brackets {i}. For the two **independent groups of parameters** in contrast, each value of the first parameter group will be combined with each value of the second parameter group. For example, if each of the parameters in the first

independent group has 5 values assigned `sweep.values_1{1}=[v1 v2 v3 v4 v5]`, and 4 in the second independent group `sweep.values_2{1}=[v6 v7 v8 v9]`, a total of $5 \times 4 = 20$ simulations will be performed. Either of the two independent groups can be disabled by assigning an empty matrix to its values, e.g. for disabling the second group: `sweep.values_2{1}=[]`.

Sweep parameter can be any parameter assigned in the settings file, with the exception of some parameters with string values, in particular external filenames.

If the parallel mode is in, a sweep will be simulated in parallel, see [Command Line Options](#).

6.2.2 OPTIMIZER

Inbuilt in Quokka is a generic optimizer algorithm, essentially using *Matlab's* bounded nonlinear optimizer algorithm's, which allows to fit unknown input parameter(s) to known output characteristics. For a successful optimization, a careful setup is required as with any other such complex function to optimize, see [Optimizer](#).

There are two different optimizer modes. **Mode 1** allows to define multiple goal values to achieve, or one goal to maximize / minimize. For a *minimize* / maximize goal the number of unknown parameters can be more than one. Otherwise the number of unknown parameters have to be equal or less than the number of goals, where in the latter case least-square fitting is performed rather than attempting exact goal achievement. **Mode 2 performs curve fitting**, where the simulated curve will be fitted by least squares to a user-defined curve. This is most commonly done in conjunction with curve terminal conditions to produce the desired curve (IV, effective lifetime curve by *suns-Voc*, to), while the sweep functionality can also be used to produce the desired curve.

Another functionality within the optimizer is given by the '**override parameters**'. This is needed when other **input parameters are dependent on the unknown parameter**, and need therefore be adjusted during the iterative optimization. For example, if one wanted to fit front and rear J_0 of a symmetric lifetime structure, one would define only the front J_0 as the unknown parameter, and override the rear J_0 with the front J_0 to ensure a symmetric structure for each simulation.

A second application for those overrides is to invoke '**sequential optimization**' to perform multiple identical optimization tasks with different conditions. In the above example, one might want to investigate the influence of the wafer thicknesses on the derived J_0 . For this, the override can be used to assign multiple values to any input parameter other than the unknown one, and Quokka will perform the defined optimization for each of those values. Alternatively / additionally start, bound and goal inputs can be assigned multiple values (with the same number) to perform sequential optimization. Note that sequential optimization can NOT be invoked by the sweep functionality, as the optimizer is implemented 'on top'. Such a sequential optimization is performed in parallel, when the parallel mode is on, see [Command Line Options](#).

7. TROUBLESHOOTING / FAQs

Table 6: Common problems with suggested solutions and / or explanations

Problem / question	Solution / description
Inconsistent $n_{i,eff}$ and J_0	<p>While (bulk-) $n_{i,eff}$ does actually have little direct impact on most important results like IV-characteristics, it can indirectly show large influence in combination with "J_0" boundary recombination. The user must take care that a consistent assumption for $n_{i,eff}$ for both deriving J_0 and for the subsequent device simulation is used. J_0 values can often be adjusted to a different $n_{i,eff}$ by the assumption of $J_0/n_{i,eff}^2 = \text{const}$, well valid for diffusions.</p> <p>As the most prominent example, the Excel spreadsheets on Sinton lifetime testers typically assume $n_{i,eff} = 8.6 \times 10^9 \text{ cm}^{-3}$ when calculating J_0 values, which results in ca. 30% underestimation of recombination when the same J_0 values and default $n_{i,eff}$ settings in Quokka are used at 300K.</p>

Quokka stuck / bad or no convergence In estimated 95% of cases this is caused by a mistake in the settings or by setting very untypical conditions for a solar cell, not being reported by Quokka as such. Below is a list of common cases leading to convergence problems. If you still think Quokka should be able to solve your setup, please contact support@pvlighthouse.com.au.

Wrong unit of J_0 : factor 1e-15 might be missing (#1 mistake!)

Voltage too low: see [Short-circuit Limitations](#)

Mesh size too large: check the geometry using the GUI, Quokka should well handle at least 20.000 elements on standard PC's; accidental definition very small features can also cause numerical problems

High external resistance for OC conditions: unlike PC1D, Quokka does NOT require high series resistance and / or contact resistance to achieve OC conditions, this can rather cause numerical problems; Quokka iteratively takes care of accurate OC conditions

Parallel mode on: Messaging is reduced when using the parallel mode; try starting the simulation in the non-parallel mode and Quokka might tell you what's wrong

No contacts defined: Quokka always requires the existence of contact of both polarities, however they can be set effectively "virtual" to simulate non-contacted samples, see [Meshing Insights](#).

Accidental extreme conditions within a sweep: When setting up a large parameter sweep, it often results in some particular parameter combination representing extreme conditions which are hard to solve.

Optimizer stuck: As with any such complex and strongly non-linear optimization task, an educated setup of the problem is crucial for successful convergence, see [Optimizer](#).

Cryptic error message Not being the fun part and lacking commitment within a free tool, the implementation of error handling is far from comprehensive and a "cryptic error message" is the dominant behaviour when something goes wrong. Mostly this is due to errors in the settings file. If you created / changed it manually, a convenient way for a sanity check is uploading it to the settings file generator, which might find and fix wrong or missing assignments. If you can't find anything wrong with your settings file, please send it to support@pvlighthouse.com.au.

Should I use 'S' or ' J_0 ' model for surface recombination? Which model is more appropriate is up to the user to decide and depends on the detailed physics within the near-surface region. As a simple guide, most highly doped regions or highly charged surfaces follow a J_0 recombination, while some passivated surfaces are well approximated by an effective surface recombination velocity. In low injection, both models yield equivalent results. For low and moderately charged surfaces, neither of the two models may be applicable, and an analytic expression for the actual injection dependence needs to be used.

What exactly do the inputs `suns` and `intensity` do? Once a generation profile is defined by either of the generation types, it is scaled by the user input for `suns`, which therefore effectively states a scaling factor. However, further influence is given on the post-calculated efficiency as it also scales the intensity.

The user input for intensity does have no influence on the generation. It is solely required to post-calculate the efficiency. Furthermore, the intensity user input will be disregarded in the '1D_model', as it is then defined by the chosen spectrum. The formula below highlights the influence of `suns` and `intensity` on the efficiency:

$$\text{efficiency} = \text{terminal power} / (\text{intensity} \times \text{suns})$$

A complication arises when one wants to scale an external generation profile to fit a desired current. Using the `suns`-value does this job, but also scales the intensity for calculating the efficiency, which is consequently not the desired (but physical correct) value. Therefore `suns` should not be used for this purpose, but rather `generation.Jgen_correction` should be enabled with the desired generation current defined as `generation.Jgen`.

8. QUOKKA PHYSICS OVERVIEW

© 2014 Andreas Fell

Quokka numerically solves the 1D/2D/3D steady-state charge carrier transport in a quasi-neutral silicon device in an efficient and fast manner. It uses so called 'conductive boundaries' to account for increased lateral conductivity in near surface regions (e.g. diffusion or inversion layer) and thus to simulate most silicon solar cell devices without major loss of generality. This page summarizes the implemented models and material properties.

8.1 CHARGE CARRIER TRANSPORT MODEL

The equations here are shown for a p-type bulk as an example, and can be analogously derived and applied for an n-type bulk.

8.1.1 VOLUMETRIC (BULK) EQUATIONS

The basic equations solved in Quokka are a simplified set of two differential equations describing the steady-state charge carrier transport in a quasi-neutral semiconductor. The variables to solve for are the quasi-Fermi potentials of electrons and holes φ_{Fn} and φ_{Fp} respectively.

$$\nabla (\sigma_n \nabla \varphi_{Fn}) = q (G - R) \quad (1)$$

$$\nabla (\sigma_p \nabla \varphi_{Fp}) = -q (G - R) \quad (2)$$

The conductivities and the recombination rate in general is a function of the carrier density. They can be derived from the quasi-Fermi potentials by the quasi-neutrality condition $p \approx n + N_A - n_0$ and equation (18) to [1]:

$$n = -\frac{N_A - n_0}{2} + \sqrt{\frac{(N_A - n_0)^2}{4} + n_{i,eff}^2 \exp\left(\frac{\varphi_{Fn} - \varphi_{Fp}}{V_T}\right)} \quad (3)$$

8.1.2 BOUNDARY CONDITIONS

Boundary recombination

For both conductive and non-conductive boundaries, the recombination current at or into the boundary is evaluated by either a J_{01}/J_{02} model, S model, or a user-defined analytic expression.

$$J_{rec,J0} = J_{01} \left(\frac{np}{n_{i,eff}^2} - 1 \right) + J_{02} \left(\sqrt{\frac{np}{n_{i,eff}^2}} - 1 \right) \quad (4)$$

$$J_{rec,S} = S(n - n_0)q \quad (5)$$

$$J_{rec,an} = f(n, p, \dots) \quad (6)$$

Symmetry boundaries

At the symmetry boundaries, i.e. all boundaries except the front and the rear side, the component of the gradient of the quasi-Fermi potentials in direction of the surface normal, defined by the normal vector \vec{n} , is zero:

$$\vec{n} \nabla \varphi_{Fn/p} = 0 \quad (7)$$

Non-conductive boundaries

The electron current equals the negative recombination current:

$$\sigma_n \vec{n} \nabla \varphi_{Fn} = -J_{rec} \quad (8)$$

At non-contacted regions the total current into the boundary needs to be zero:

$$\sigma_n \vec{n} \nabla \varphi_{Fn} + \sigma_p \vec{n} \nabla \varphi_{Fp} = 0 \quad (9)$$

An electrical contact with the voltage V at the non-conductive boundaries is included by setting the current density through the contact resistance r_c equal to the total current density at the boundary:

$$\sigma_n \vec{n} \nabla \varphi_{Fn} + \sigma_p \vec{n} \nabla \varphi_{Fp} = \frac{V - \varphi_{Fp}}{r_c} \quad (10)$$

At regions without external contacts the contact resistance becomes infinite and sets the total current density into the boundary consistently to zero. Care should be taken when simulating a lowly recombining contact, as the quasi-neutrality approximation is not valid when significant currents are extracted and can thus result in significant errors.

Note that this implementation of the contact resistance, also in case of a conductive boundary, accounts correctly for current transfer effects into the contacts.

Conductive boundaries

The conduction of carriers in a conductive layer at the surface (e.g. diffusion or inversion layer) is accounted for by a 2D continuity equation of the majority quasi-Fermi potential φ_{Fdiff} with the sheet resistance R_{sheet}

$$\nabla_t \left(\frac{1}{R_{sheet}} \nabla_t \varphi_{Fdiff} \right) = J_{diff} \quad (11)$$

For a n-type conductive boundary (emitter) this gives the boundary condition for the bulk electron quasi-Fermi potential:

$$\varphi_{Fn} = \varphi_{Fdiff} \quad (12)$$

The source term J_{diff} equals the total current density from the base into the emitter less the current density into the contact:

$$J_{diff} = \sigma_n \vec{n} \nabla \varphi_{Fn} + \sigma_p \vec{n} \nabla \varphi_{Fp} - \frac{V - \varphi_{Fdiff}}{r_c} \quad (13)$$

The hole current density into the boundary equals the recombination current density less the current density generated within the boundary J_G times its collection efficiency η_{coll} , which gives the boundary condition for the hole quasi-Fermi potential:

$$\sigma_p \vec{n} \nabla \varphi_{Fp} = J_{rec} - J_G \eta_{coll} \quad (14)$$

For a p-type diffusion (back surface field) the expressions are equivalent with altered carrier types and an inverted sign of the recombination current density.

8.2 SILICON PROPERTIES

8.2.1 BAND STRUCTURE AND INTRINSIC CARRIER DENSITY

The effective band gap energy is calculated by a temperature dependent $E_{g,0}$ and a doping dependent band gap narrowing (BGN) ΔE_g .

$$E_{g,eff} = E_{g,0} - \Delta E_g \quad (15)$$

ΔE_g is determined by a lookup table with values derived from [2] which considers a doping dependence at 300 K only, i.e. representing the curve in Fig. 9 of [2].

To calculate carrier densities Boltzman statistics are assumed. This is valid as Quokka solves only in the relatively lowly doped bulk, where the difference to Fermi-Dirac statistics is negligible.

$$n = N_c \exp \left(\frac{\varphi_n + \varphi_e}{V_T} \right) \quad (16)$$

$$p = N_v \exp \left(\frac{-\varphi_p - \varphi_e}{V_T} - \frac{E_{g,eff}}{kT} \right) \quad (17)$$

Here φ_n and φ_p are the electron and hole quasi-Fermi potentials, N_c and N_v the density of states (DOS) in the conduction

and valence band respectively, and $V_T = kT/q$ the thermal voltage. Note that what is denoted as the electric potential φ_e is more accurately the conduction band edge potential, which differs to the electric potential by the electron affinity and the reference electric potential.

It follows the well-known relation between pn product and Fermi-level splitting which is applied to solve the bulk carrier transport, with the effective intrinsic carrier density $n_{i,eff}^2$ being the only decisive value for accurate modelling of carrier transport.

$$pn = n_{i,eff}^2 \exp\left(\frac{\varphi_n - \varphi_p}{V_T}\right) \quad (18)$$

$$n_{i,eff}^2 = N_c N_v \exp\left(-\frac{E_{g,eff}}{kT}\right) = n_{i,0}^2 + N_c N_v \exp\left(-\frac{\Delta E_g}{kT}\right) \quad (19)$$

As default settings Quokka uses the values for DOS published by Green [3], and the temperature dependent band gap expression given in the Sentaurus user manual with slightly changed parameters to match the commonly accepted best value for the intrinsic carrier density at 300 K, $n_{i,0} = 9.65 \times 10^9 \text{ cm}^{-3}$.

$$N_c = 2.86 \times 10^{19} \left(\frac{T}{300K}\right)^{1.58} \text{ cm}^{-3} \quad (20)$$

$$N_v = 3.10 \times 10^{19} \left(\frac{T}{300K}\right)^{1.85} \text{ cm}^{-3} \quad (21)$$

$$E_{g,0} = 1.175 \text{ eV} - \frac{4.73 \times 10^{-4} \frac{\text{eV}}{\text{K}} T^2}{T + 636 \text{ K}} \quad (22)$$

8.2.2 CARRIER CONDUCTIVITY

The conductivities σ of the carriers are functions of their mobilities μ .

$$\sigma_n = qn\mu_n \quad (23)$$

$$\sigma_p = qp\mu_p \quad (24)$$

Implemented in Quokka are the mobility models by Klaassen [4] and Arora [5], where in the latter case the excess carrier density is added to the doping density to account for injection dependence, which is the way it is implemented in PC1D.

8.2.3 BULK RECOMBINATION

Quokka accounts for radiative, Auger and Shockley-Read-Hall (SRH) recombination in the bulk to calculate the recombination rate R . The sum of radiative and Auger recombination is called intrinsic recombination. The Auger models implemented in Quokka comprise the parameterizations by Kerr and Cuevas [6], Altermatt [7] and Richter et al. [8] (eq. (18) without B_{rel}), as well as the constant recombination coefficient model by Sinton and Swanson [9], which is the one used in the spreadsheet of the Sinton testers.

Implemented in Quokka is the general SRH expression:

$$R_{SRH} = \frac{np - n_{i,eff}^2}{\tau_{p0}(n_1 + n) + \tau_{n0}(p_1 + p)} \quad (25)$$

Multiple custom defects can be defined by their defect level E_t relative to the intrinsic energy E_i (approx. defined as the energy level in the middle of the effective bandgap), the capture cross sections $c_{n/p}$ and the defect density N_t , with the thermal velocity $v_{th} = 1.1 \times 10^7 \text{ cm s}^{-1}$.

$$\tau_{n0/p0} = (v_{th} c_{n/p} N_t)^{-1} \quad (26)$$

$$n_1 = n_{i,eff} \exp\left(\frac{E_t - E_i}{kT}\right) \quad (27)$$

$$p_1 = n_{i,eff} \exp\left(-\frac{E_t - E_i}{kT}\right) \quad (28)$$

Additionally a simplified midgap defect energy recombination is implemented where the user inputs τ_{p0}/τ_{n0} , and n_1/p_1 are equal to $n_{i,eff}$.

As a further contribution is given by the boron-oxygen recombination in p-type material as given by Altermatt [7], where the user needs to set the oxygen concentration $N_{t,0}$ and a processing dependent parameter m while the boron concentration is given by the doping density N_A and the energy level is 0.41 eV below the conduction band edge.

$$\tau_{n0,BO} = 4.02024 \times 10^{45} N_A^{-0.824} N_{t,0}^{-1.748} m \quad (29)$$

$$\tau_{p0,BO} = 10\tau_{n0,BO} \quad (30)$$

total bulk recombination is then calculated as the sum of all contributions, where each contribution can be either switched off, or needs to be assigned very high lifetime values to effectively disable:

$$R = \sum R_{SRH,custom} + R_{SRH0} + R_{SRH,BO} + R_{Auger} + B_{rad}pn + \tau_{b,fixed}(n - n_0) \quad (31)$$

8.2.4 OPTICAL ABSORPTION

Wavelength dependent refractive index / absorption data is required for determining the generation profile when the '1D_model' is used, as well as for re-absorption within luminescence modelling. By default, Quokka uses the optical properties of silicon from Nguyen [10], and combines it with the data from Green [11] to cover the full wavelength range. Quokka incorporates the published temperature dependence for deriving optical properties at arbitrary temperatures. As a further option, which is prominently used in literature and other software tools, the data from Green [11] fixed at 300K can be set.

8.3 OPTICAL MODELLING BY '1D_MODEL'

Quokka's focus is on the simulation of carrier transport and excludes the capability to perform optical modelling from physical optical properties of the cell and consequently derive the required generation profile. There are several options to define generation, comprising the direct definition of the generation profile by the user, a user-defined generation current, and a one-dimensional model accounting for wavelength-dependent effective properties, which was published in [12].

The one-dimensional model '**1D_model**' derives a generation profile from a defined spectrum, front transmission $T_{front}(\lambda)$ and pathlength enhancement $Z(\lambda)$. Note that those inputs already define the total generation current (for a given wafer thickness W_z and refractive index data of silicon). Consequently total generation can be considered a user-input rather than a quantity modelled by Quokka, which ensures consistency with for example raytracing programs when deriving the required inputs. Furthermore, the facet angle of the front surface texture must be given, which is zero for a planar surface.

For each wavelength bin (5nm in Quokka), the incoming photon flux $N_{ph}(\lambda)$ is derived from the incident spectrum. Each monochromatic ray is then traced through the wafer accounting for its angle to enhance its travel length and absorption. For a textured surface, a different angle is applied inside and outside of the junction depth as suggested in [13], see figure below. After traveling to the rear of the wafer, the remaining absorption from the difference of total pathlength and first-pass pathlength is equally distributed throughout the thickness of the device. It has been found that this model provides high accuracy for wafer-based silicon solar cells.

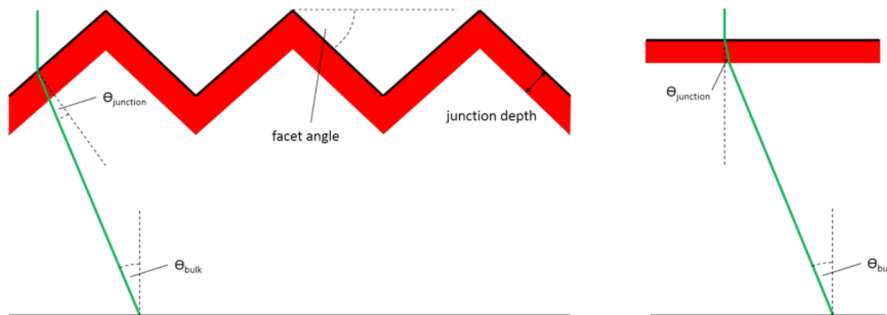


Figure 7: Illustration of '1D_model' generation calculation; left: textured case; right: 1D representation.

8.4 FREE ENERGY LOSS ANALYSIS (FELA)

The free energy loss analysis (FELA) as comprehensively described in [14] is implemented in Quokka. It enables to compare resistive losses and recombination losses in the common power loss unit mW/cm². Incidentally, for the typical 100 mW/cm² incident light intensity, the power loss values are equivalent to efficiency loss in %abs.

A drawback of the FELA is that recombination losses are in general underestimated, as they are a function of quasi-Fermi level splitting, which in turn is a result of recombination. The losses add up to the generated power density, which is also a function of quasi-Fermi level splitting and therefore overall recombination. Effectively, the part of the entropy loss which is caused by avoidable recombination is missing in FELA when aiming for a loss breakdown towards the Auger-Limit [15]. However, FELA is very suitable to identify the main resistive and recombination loss contributions and the potential for incremental efficiency improvements. Table 1 summarizes the expressions used for the different loss contributions considered in Quokka.

A notable quantity Quokka calculates is the FELA balance ε_{FELA} . Mathematically the output power must equal the generated power less the sum of the FELA contributions. The FELA balance gives a metric how close this is numerically achieved, and is consequently a useful indicator for the consistency and accuracy of the numerical solution to the carrier transport equations. See the user manual for details on how this should be interpreted. It is defined as

$$\varepsilon_{FELA} = \frac{\text{generated power} - \text{sum of FELA (excluding external losses)} - V_{uc}J_{uc}}{\max(\text{generated power}, V_{uc}J_{uc})} \quad (32)$$

Table 7: FELA expressions; A denotes the lateral (xy) solution domain area, $\Delta\varphi$ the splitting of quasi-Fermi potentials, dV volume integration and dA boundary integration

FELA name / comment	Equation
generated power	$A^{-1} \iiint G \Delta\varphi dV$
bulk recombination loss	$A^{-1} \iiint R \Delta\varphi dV$
boundary recombination loss including suboptimal collection efficiency loss for conductive boundaries	$A^{-1} \iint (J_{rec} + J_G(1 - \eta_{coll})) \Delta\varphi dA$
bulk electron resistive loss	$A^{-1} \iiint \vec{J}_{bulk,n} ^2 / \sigma_n dV$
bulk hole resistive loss	$A^{-1} \iiint \vec{J}_{bulk,p} ^2 / \sigma_p dV$
conductive boundary resistive loss note that boundary current density has units of A/m, opposed to A/m ² in the bulk	$A^{-1} \iint \vec{J}_{bound} ^2 R_{sheet} dA$
contact resistance loss takes current transfer effects into account	$A^{-1} \iint (\varphi_{diff} - V)^2 / r_c dA$
external shunt resistance loss	V_{uc}^2 / R_{shunt}
external series resistance loss	$J_{term}^2 R_{series}$
external diode loss	$V_{uc} J_D$

8.5 LUMINESCENCE MODELLING

8.5.1 FUNDAMENTAL EQUATION

Quokka 2.0 simulates the detected luminescence map by integrating over the z axis of the simulated device:

$$PL_{det}(x, y) = \int_0^W \int_{800 \text{ nm}}^{1400 \text{ nm}} r_{sp}(x, y, z, \lambda) f_{esc}(x, y, z, \alpha_{Si}) \phi(\lambda, t, \alpha_{Si}) d\lambda dz \quad (33)$$

where r_{sp} is the rate of spontaneous emission via band-to-band transitions in silicon, f_{esc} the escape function defining the probability that a photon will be emitted from the device and ϕ the detector sensitivity. As Quokka separates the electrical and optical simulations, luminescence maps can be produced under either photoluminescence or electroluminescence conditions. Each component of Equation (31) is described in detail in the subsequent sections.

8.5.2 SPONTANEOUS EMISSION SPECTRUM

The rate of spontaneous emission via band-to-band transitions is calculated using the generalized form of Planck's Law as described by Wurfel [16]. The rate of spontaneous emission (in units of photons nm⁻¹ s⁻¹ cm⁻²) emitted isotropically into 4π steradians is expressed as:

$$dr_{sp}(x, y, z, \lambda) = \alpha_{Si}(\lambda) BB(\lambda, T) \exp \left[\frac{\Delta\eta(x, y, z)}{kT} \right] d\lambda \quad (34)$$

where $\alpha_{Si}(\lambda)$ is the wavelength-dependent absorption coefficient of silicon, $BB(\lambda, T)$ the black-body photon flux and $\Delta\eta(x, y, z)$

$= \varphi_{Fn} - \varphi_{Fp}$ the local separation of the quasi-Fermi energies. Quokka employs the optical data of Daub over the wavelength range of the emission spectrum of silicon as it has demonstrated the best fit to experiment [17]. The electronic simulation of Quokka calculates the local splitting of the quasi-Fermi potential for every element of the device and from Equation (32), an accompanying radiative emission rate, an example of which is produced in the figure below.

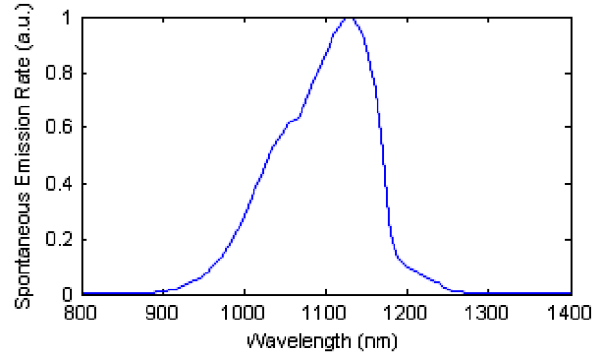


Figure 8: Emission spectrum.

This spectrum, however, is not what is ultimately emitted from the silicon wafer or solar cell, which is determined by the optical losses within the structure.

8.5.3 THE ESCAPE FUNCTION F_{ESC}

Numerous so-called emission functions exist in literature. Several [18-20] have been implemented in Quokka. These functions describe the probability with which a spontaneously emitted photon will escape from the emitting medium without being 'lost', either to reabsorption or total internal reflection.

In the case of perfectly planar devices, only a relatively small proportion of emitted photons fall within the narrow escape-cone that is determined by the relative refractive indices of the emitting and ambient media. In Quokka, it is assumed that the device is in an air ambient ($n_{air}(\lambda) = 1$), and the fraction $1/n_{Si}^2$ of total emitted photons falls within the escape cone.

If the device surfaces are perfectly planar and parallel, the photons incident on the silicon-air interface beyond the escape cone are totally internally reflected and assumed to be unavailable to an external detector. However, not all photons within the escape cone will be transmitted on their first interaction with the wafer surface and are instead reflected internally. Owing to subsequent internal reflections these photons will have a further opportunity to be emitted from the front surface of the device, but on each pass will be attenuated by reabsorption in the silicon bulk modeled after Beer-Lambert absorption. This brings us to the escape function proposed by Schick [18], which is implemented in Quokka to describe the emitted luminescence flux for planar devices.

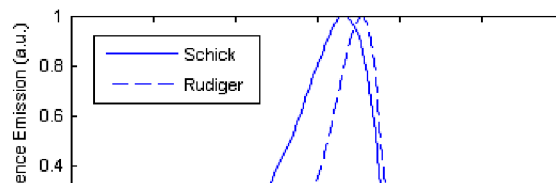
$$f_{esc}(z, \lambda) = [1 - R_f] [\exp(-\alpha_{Si}z) + R_b(-\alpha_{Si}(2W - z))] \frac{1}{1 - R_f R_b \exp(-2\alpha_{Si}W)} \quad (35)$$

It has been noted by Schinke *et al.* [20] that the escape function of Equation (33) is functionally equivalent to those described by Green [21], Daub [22] and Trupke [23], and thus is representative of a function broadly used in the PV literature.

Quokka also includes escape functions that account for diffuse and/or specularly reflecting surfaces. The model of Rudiger *et al.* [19] assumes that the front and rear surfaces of the device are fully diffuse reflectors, as might be encountered with front and rear textured devices. The escape function is described by:

$$f_{esc}(z) = \left[1 + \left(1 - \frac{1}{n_{Si}^2} \right) \right] \exp[-4\alpha(W - z)] \exp[-2\alpha z] \sum_{i=0}^{\infty} \left(1 - \frac{1}{n_{Si}^2} \right)^{2i} \exp(-4i\alpha d) \quad (36)$$

The figure below plots the emitted luminescence spectrum simulated by Quokka for the escape functions of Schick and Rudiger.



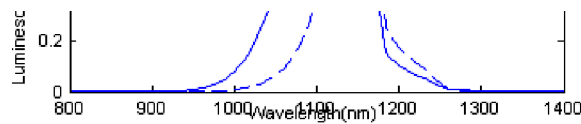


Figure 9: Emission spectra modelled after the escape functions of Schick and Rudiger.

A more general escape function has been developed by Schinke *et al.* [20], which describes the probability of photon emission for any combination of planar (specular) and textured (diffuse) reflecting surfaces. It contains the functions of Schick and Rudiger as special cases, determined by appropriate input variables. It has been implemented in Quokka, with the functions of Schick and Rudiger retained for the relative ease of use. For details on the general emission function, refer to [20], which also provides a valuable overview of escape functions employed in the PV literature.

It is important to note that the above escape functions are statistical predictions of emission, and **do not account for the spatial distribution** of the emitted photons. Thus, luminescence maps, particularly in the case of diffusely reflecting samples, need to be interpreted with caution. Quokka assumes that the emitted photons are constrained within the z-axis of the element from which they are emitted.

8.5.4 GEOMETRICAL BLURRING MODEL

To address this last mentioned limitation, the geometrical blurring model by Padilla *et al.* [24] is implemented in Quokka and can be chosen instead of the escape functions. It assumes both the front and the rear internal surfaces to be Lambertian reflectors. Note that it requires a relatively fine lateral mesh to give accurate and smooth results, which, in particular in 3D, can be highly computationally expensive.

8.5.5 THE DETECTION FUNCTION ϕ

The detection function describes the wavelength-dependent external quantum efficiency (EQE) of the imaging sensor, including the presence of any short or long-pass filters. The response is modelled after Beer-Lambert absorption assuming perfect collection efficiency for absorbed photons. Quokka will determine the QE for a silicon-based detector of user-defined thickness, or will accept a definition of the sensor's EQE via an external excel spreadsheet.

8.6 EXTERNAL CIRCUIT

Below is a sketch of the external circuit elements and current directions. The convention is that a positive unit cell voltage V_{uc} in dark condition results in a positive unit cell current J_{uc} , regardless of whether it is a n-type or p-type solar cell, and V_{uc} is applied to the contact of opposite polarity to the bulk. The external diode is in forward bias and its current is given by the saturation current density J_{0D} and the ideality factor n_D .

$$J_D = J_{0D} \left[\exp \left(\frac{V_{uc}}{n_D V_T} \right) - 1 \right] \quad (37)$$

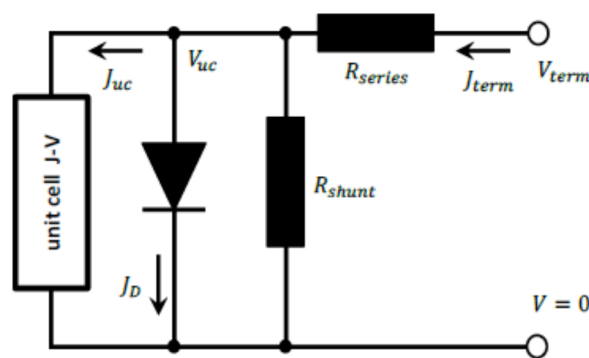


Figure 10: External circuit model.

8.7 QUANTUM EFFICIENCY

Quokka has an inbuilt algorithm to derive a biased quantum efficiency curve. First, using the bias illumination only, short circuit current conditions are searched for iteratively. Note that this does not mean actual short circuit conditions, but searching for a higher unit cell voltage which still results in a negligible difference of extracted current to short circuit current $J_{sc,bias}$, which is usually the case up to a couple of 100 mV. The reason for this is to prevent numerical inaccuracies, which can be significant at actual short circuit. This so derived unit cell voltage is used as a fast to solve for fixed terminal condition for the following simulations. A monochromatic illumination is then added with a photon flux representing a

small fraction of the bias generation current $J_{ph}=0.005 J_{gen,bias}$ and a sweep of the wavelength results in a wavelength dependent short circuit current $J_{sc}(\lambda)$.

The fundamental quantum efficiency characteristic Quokka simulates is the collection efficiency $CE(\lambda)$, which is largely independent of the optical properties of the device. The other more common characteristics internal and external quantum efficiency $IQE(\lambda)$ and $EQE(\lambda)$ are essentially derived from the collection efficiency by the optical input parameters front surface transmission T_{front} and pathlength enhancement $Z(\lambda)$. The respective formulas are given below, with the effective transmission $T_{eff}(\lambda)$ being defined as the (unshaded) front transmission times the unshaded area fraction $T_{eff}(\lambda) = T_{front}(\lambda) A_{unshaded}/A_{total}$:

$$CE(\lambda) = \frac{J_{sc}(\lambda) - J_{sc,bias}}{J_{gen}(\lambda) - J_{gen,bias}} \quad (38)$$

$$EQE(\lambda) = \frac{J_{sc}(\lambda) - J_{sc,bias}}{J_{ph}} \quad (39)$$

$$IQE(\lambda) = \frac{EQE(\lambda)}{T_{eff}(\lambda)} \quad (40)$$

8.8 REFERENCES

- [1] A. Fell, "A free and fast three-dimensional/two-dimensional solar cell simulator featuring conductive boundary and quasi-neutrality approximations," *IEEE Transactions on Electron Devices*, **60**, pp. 733-738, 2013.
- [2] A. Schenk, "Finite-temperature full random-phase approximation of band gap narrowing for silicon device simulation," *Journal of Applied Physics*, **84**, pp. 3684-3695, 1998.
- [3] M.A. Green, "Intrinsic concentration, effective densities of states, and effective mass in silicon," *Journal of Applied Physics*, **67**, pp. 2944-2954, 1990.
- [4] D.B.M. Klaassen, "A unified mobility model for device simulation - I. Model equations and concentration dependence," *Solid-State Electronics*, **35**, pp. 953-959, 1992.
- [5] N.D. Arora, J.R. Hauser and D.J. Roulston, "Electron and hole mobilities in silicon as a function of concentration and temperature," *IEEE Transactions on Electron Devices*, **29**, pp. 292-295, 1982.
- [6] M.J. Kerr and A. Cuevas, "General parameterization of Auger recombination in crystalline silicon," *Journal of Applied Physics*, **91**, pp. 2473-2480, 2002.
- [7] P.P. Altermatt, "Models for numerical device simulations of crystalline silicon solar cells - a review," *Journal of Computational Electronics*, **10**, pp. 314-330, 2011.
- [8] A. Richter, S.W. Glunz, F. Werner, J. Schmidt and A. Cuevas, "Improved quantitative description of Auger recombination in crystalline silicon," *Physical review B*, **86**, 165202, 2012.
- [9] R.A. Sinton and R.M. Swanson, "Recombination in highly injected silicon," *IEEE Transactions on Electron Devices*, **34**, pp. 1380-1389, 1987.
- [10] H. T. Nguyen, F. E. Rougieux, B. Mitchell, and D. Macdonald, "Temperature dependence of the band-band absorption coefficient in crystalline silicon from photoluminescence," *Journal of Applied Physics*, **115**, pp. -, 2014.
- [11] M.A. Green, "Self-consistent optical parameters of intrinsic silicon at 300 K including temperature coefficients," *Solar Energy Materials and Solar Cells*, **92**, pp. 1305-1310, 2008.
- [12] A. Fell and K. R. McIntosh, "Deriving the generation profile for silicon solar cells from lumped optical parameters," in 42nd IEEE Photovoltaic Specialists Conference, New Orleans, USA, 2015.
- [13] P. A. Basore, "Numerical modeling of textured silicon solar cells using PC-1D," *Electron Devices, IEEE Transactions on*, vol. 37, pp. 337-343, 1990.

- [14] R. Brendel, S. Dreissigacker, N. P. Harder, and P. P. Altermatt, "Theory of analyzing free energy losses in solar cells," *Applied Physics Letters*, vol. 93, pp. 173503-173503-3, 2008.
 - [15] J. Greulich, H. Höffler, U. Würfel, and S. Rein, "Numerical power balance and free energy loss analysis for solar cells including optical, thermodynamic, and electrical aspects," *Journal of Applied Physics*, vol. 114, pp. -, 2013.
 - [16] P. Würfel, S. Finkbeiner and E. Daub, "Generalized Planck's radiation law for luminescence via indirect transitions," *Applied Physics A*, **60**, pp. 67-70, 1995.
 - [17] B. Mitchell, M.K. Juhl, M.A. Green and T. Trupke, "Full spectrim photoluminescence lifetime analysis on silicon bricks," *IEEE Journal of Photovoltaics*, **3**, pp. 962-969, 2013.
 - [18] K. Schick, E. Daub, S. Finkbeiner and P. Würfel, "Verification of a generalized Planck law for luminescence radiation from silicon solar cells," *Applied Physics A*, **54**, pp. 962-969, 2013.
 - [19] M. Rudiger, T. Trupke, P. Würfel, T. Roth and S.W. Glunz, "Influence of photon reabsorption on temperature dependent quasi-steady-state photoluminescence lifetime measurements on crystalline silicon," *Applied Physics Letters*, **92**, 222112, 2008.
 - [20] C. Schinke, D. Hinken, J. Schmidt, K. Bothe and R. Brendel, "Modeling the spectral luminescence emission of silicon solar cells and wafers," *IEEE Journal of Photovoltaics*, **3**, pp. 1038-1052, 2013.
 - [21] M.A. Green, "Analytical expressions for spectral composition of band photoluminescence from silicon wafers and bricks," *Applied Physics Letters*, **99**, 131112, 2011.
 - [22] E. Daub and P. Würfel, "Ultra-low values of the absorption coefficient for band-band transitions in moderately doped Si obtained from luminescence," *Journal of Applied Physics*, **80**, pp. 5325-5331, 1996.
 - [23] T. Trupke, E. Daub and P. Würfel, "Absorptivity of silicon solar cells obtained from luminescence," *Solar Energy Materials and Solar Cells*, **53**, pp. 103-114, 1998.
 - [24] M. Padilla, H. Höffler, C. Reichel, H. Chu, J. Greulich, S. Rein, W. Warta, M. Hermle, and M. C. Schubert, "Surface recombination parameters of interdigitated-back-contact silicon solar cells obtained by modeling luminescence images," *Solar Energy Materials and Solar Cells*, **120**, pp. 363-375, 2014.
-